

# The HP1–p150/CAF-1 interaction is required for pericentric heterochromatin replication and S-phase progression in mouse cells

Jean-Pierre Quivy<sup>1,2</sup>, Annabelle Gérard<sup>1,2</sup>, Adam J L Cook<sup>1</sup>, Danièle Roche<sup>1</sup> & Geneviève Almouzni<sup>1</sup>

**The heterochromatin protein 1 (HP1)-rich heterochromatin domains next to centromeres are crucial for chromosome segregation during mitosis. This mitotic function requires their faithful reproduction during the preceding S phase, a process whose mechanism and regulation are current puzzles. Here we show that p150, a subunit of chromatin assembly factor 1, has a key role in the replication of pericentric heterochromatin and S-phase progression in mouse cells, independently of its known function in histone deposition. By a combination of depletion and complementation assays *in vivo*, we link this unique function of p150 to its ability to interact with HP1. Absence of this functional interaction triggers S-phase arrest at the time of replication of pericentromeric heterochromatin, without eliciting known DNA-based checkpoint pathways. Notably, in cells lacking the histone methylases Suv39h, in which pericentric domains do not show HP1 accumulation, p150 is dispensable for S-phase progression.**

Genomic DNA in the nucleus of a eukaryotic cell is packaged into chromatin, a nucleoprotein complex, whose fundamental unit is the nucleosome. This basic building block consists of a core particle (146 base pairs of DNA wrapped around a histone octamer<sup>1</sup>) and linker DNA. Additional chromatin proteins and further folding of the nucleosomal template contribute to the formation of specific chromatin domains such as those corresponding to centromeric heterochromatin, which are crucial for genome stability<sup>2,3</sup>. This is exemplified in mouse cells by the high accumulation of HP1 isoforms at constitutive heterochromatin domains<sup>4</sup>. These regions located next to centromeres, called pericentric heterochromatin, are critical for proper chromosome segregation<sup>5</sup>. They consist of repetitive major satellite (pericentric) DNA sequences and flank repetitive minor satellite (centric) DNA sequences<sup>6</sup>. Notably, in mouse cells, the clustering in interphase of major satellite repeats from individual chromosomes forms distinct entities easily detected by DAPI (4,6-diamidino-2-phenylindole) staining<sup>5,7</sup>. Therefore, maintenance and accurate reproduction of such a complex heterochromatin structure throughout multiple cell divisions represents a major challenge to ensure its stability.

Inheritance of functional centromeres demands that, during S phase, not only does DNA need to be replicated but, concomitantly, each replicated daughter strand should be incorporated into a whole domain with its special architecture. These two requirements necessitate both disruption and assembly events, not simply of nucleosomal organization but also of higher-order structures involving the displacement or incorporation of associated proteins such as HP1. At the nucleosomal level, replication fork passage displaces parental histones

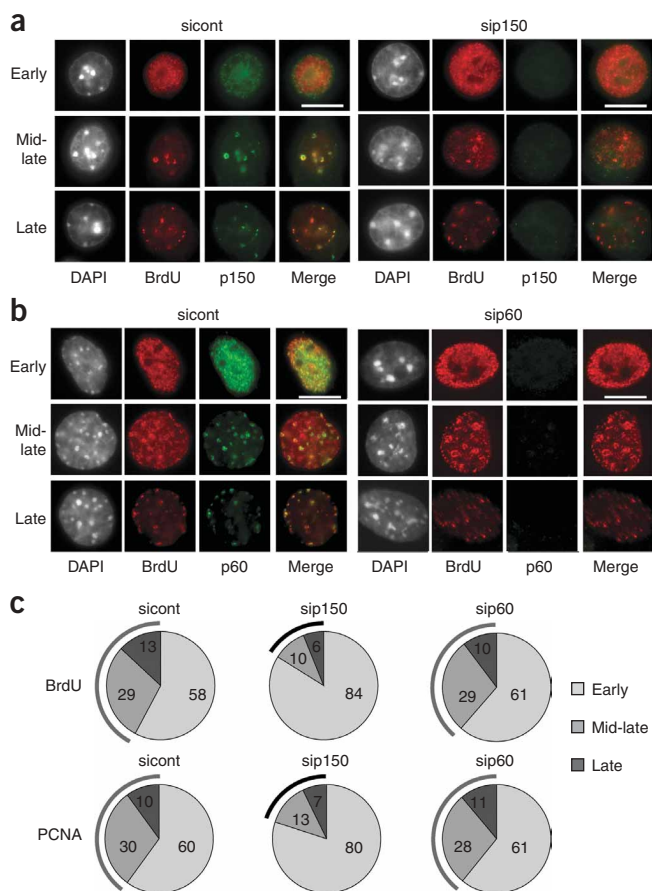
ahead of the replication fork. Redistribution of the evicted histones on the two daughter strands in combination with deposition of newly synthesized histones provides a full nucleosome complement for the newly replicated DNA<sup>8</sup>.

Increasing knowledge about histone dynamics and associated chaperones has improved our understanding of histone displacement and incorporation<sup>9,10</sup>. However, in the case of the complex organization of constitutive heterochromatin, the mechanisms by which HP1 proteins are displaced and reassociated during replication fork passage are poorly understood. Fluorescence recovery after photobleaching (FRAP) experiments have indicated that HP1 binding dynamics differ in euchromatin and heterochromatin<sup>11,12</sup>. However, how HP1 dynamics can be controlled to avoid defects in reproduction of the chromatin structure during replication of pericentric heterochromatin is an enigma. This is of critical importance given that centromere identity and function has long been known to be epigenetically specified by the chromatin structure in particular, rather than by the DNA sequence itself<sup>13</sup>. Furthermore, in *Schizosaccharomyces pombe*, the identity of centromeric regions depends on the organization of adjacent pericentric heterochromatin<sup>14</sup>. To coordinate reproduction of pericentric heterochromatin with a control of S-phase progression would thus be advantageous to ensure proper inheritance of these sophisticated domains.

We reasoned that, in addition to general DNA damage checkpoints, dynamics of intrinsic chromatin components within these particular domains could possibly contribute to such a control. Given the high enrichment and importance of HP1 in pericentric heterochromatin,

<sup>1</sup>Institut Curie, Centre de Recherche, UMR218 du CNRS, 26, rue d'Ulm, 75248 Paris cedex 05, France. <sup>2</sup>These authors contributed equally to this work. Correspondence should be addressed to G.A. (genevieve.almouzni@curie.fr).

Received 24 April; accepted 26 June; published online 17 August 2008; doi:10.1038/nsmb.1470



we searched for factors that could establish a link between HP1, replication and chromatin. The histone chaperone chromatin assembly factor 1 (CAF-1) was of particular interest in this context. Comprising three subunits in mammals (p150, p60 and p48)<sup>8,15</sup>, it was initially identified on the basis of its ability to specifically assemble nucleosomes *in vitro* onto newly synthesized DNA during replication<sup>16</sup>. It is found *in vivo* at replication foci<sup>17,18</sup>, and this can be accounted for by the fact that its largest subunit p150 interacts directly with PCNA<sup>19,20</sup>. In addition, the same CAF-1 subunit possesses the interesting property of directly binding to HP1 $\beta$  *in vitro*<sup>21</sup>. Structural analysis revealed that this interaction takes advantage of a key domain in p150 called the Mod-interacting region (MIR) and a cognate motif conserved in the three mammalian HP1 isoforms ( $\alpha$ ,  $\beta$  and  $\gamma$ )<sup>22</sup>. This recognition applies to the different HP1 isoforms and can explain interactions of HP1 proteins with p150 *in vivo*<sup>21</sup>, in particular the ability of p150 to stabilize a replicative pool of HP1 proteins at heterochromatin during replication<sup>23</sup>. Notably, isolation of nuclear HP1 complexes showed that they contain CAF-1 without detectable histone H3-H4 (ref. 23), and thus are distinct from H3.1 complexes in which CAF-1 is also present<sup>24</sup>. In light of this link between CAF-1, HP1 and the organization of particular replication domains, we investigated whether this sole interaction has an impact on replication progression.

We report that the largest subunit of CAF-1, p150, is uniquely required for the progression of S phase in mouse cells, independent of its ability to promote histone deposition but dependent on its ability to interact with HP1. We discuss how this HP1-CAF-1 interaction module functions as a built-in replication control for heterochromatin, which, like a control barrier, has an impact on S-phase progression in addition to DNA-based checkpoints.

**Figure 1** Depletion of p150 but not p60 leads to accumulation of cells in early S phase. **(a,b)** The pattern of BrdU incorporation (red) in S-phase cells after knockdown of individual p150 **(a)** or p60 **(b)** CAF-1 subunits (green) was revealed by immunofluorescence. In each case, control staining was performed on cells transfected with control siRNA (sicont). p150 and p60 immunostaining and BrdU incorporation are shown together with DAPI staining and merge images. The identification of early, mid-late and late S-phase patterns was based on characteristic patterns as previously defined<sup>23</sup>. The scale bar indicates 10  $\mu$ m. **(c)** Pie charts show quantitative analysis of the proportion of S-phase cells in early, mid-late and late S-phase (percentage within S phase) following transfection with control siRNA or siRNA against p150 or p60. S-phase patterns were scored by BrdU incorporation and PCNA immunostaining as indicated. Gray and black arc lines on the left of the pie charts indicate unaltered and altered proportions of mid-late and late S-phase nuclei, respectively. Numbers represent the mean of five independent experiments ( $n = 200$  S-phase nuclei by experiment) with a s.d. of  $\pm 4$  for early S phase,  $\pm 2$  for mid-late S phase and  $\pm 2$  for late S phase.

## RESULTS

### p150 but not p60 is required for S-phase progression

To dissect the cellular response to CAF-1 loss of function in mouse 3T3 cells, we examined the effect of small interfering RNA (siRNA)-mediated individual knockdown of p150 or p60 subunits. Immunofluorescence and western blot analysis showed that more than 90% of p150 and p60 were depleted 72 h after transfection with siRNA duplex (**Supplementary Fig. 1a,b** online). Remarkably, depletion of individual subunits led to the same loss of CAF-1-dependent nucleosome assembly activity, as shown by an *in vitro* supercoiling assay (**Supplementary Fig. 1c**), but the outcome in terms of cellular fate was different. The depletion of p150 alone prevented cell proliferation, and analysis of DNA content by flow cytometry revealed an accumulation of cells in S phase 48–72 h after transfection (**Supplementary Fig. 1d** and ref. 23). Beyond 72 h, we observed cell death, with an increase of cellular debris and a concomitant decrease in the number of adherent cells. This is consistent with data obtained using dominant-negative p150 or siRNA interference in human cells<sup>25,26</sup> and with a p150 conditional knockout in chicken DT40 cells<sup>27</sup>. In contrast, p60 depletion, which did not appreciably affect the level of p150 (**Supplementary Fig. 1a,b**), did not alter the cell-cycle profile (**Supplementary Fig. 1c**) and did not promote cell death, although we saw a slight decrease in cell proliferation, as reported for human cells<sup>28</sup>.

We characterized the S-phase arrest in p150-depleted cells, taking advantage of the well-defined spatiotemporal organization of sites of DNA replication (identified by bromodeoxyuridine (BrdU) incorporation and/or proliferative cell nuclear antigen (PCNA) staining) in mouse cells<sup>23,29</sup>. Following release of 3T3 cells into S phase, characteristic profiles are observed through time: first, early S-phase patterns with a high density of small foci spread throughout the nucleus; then, mid-late S-phase patterns with a typical ring-shaped labeling around pericentric heterochromatin domains; and finally, late S-phase patterns with a few large dots located mainly at the nuclear periphery<sup>23</sup> (**Fig. 1a,b**).

We first analyzed S-phase progression in control, p150- and p60-depleted cells during the time window before cell death, that is, 48–72 h after transfection (**Fig. 1a,b**). We found that the proportion of p150-depleted cells with the early S-phase pattern increased, whereas the proportions of mid-late and late S-phase cells decreased about three-fold compared to control cells (**Fig. 1c**). In contrast, p60 depletion did not alter the proportion of cells in early, mid-late and late S phase (**Fig. 1c**). Notably, inactivation of p60 did not interfere with p150 localization at sites corresponding to early, mid-late and late replication (**Supplementary Fig. 1e**), indicating that our experimental

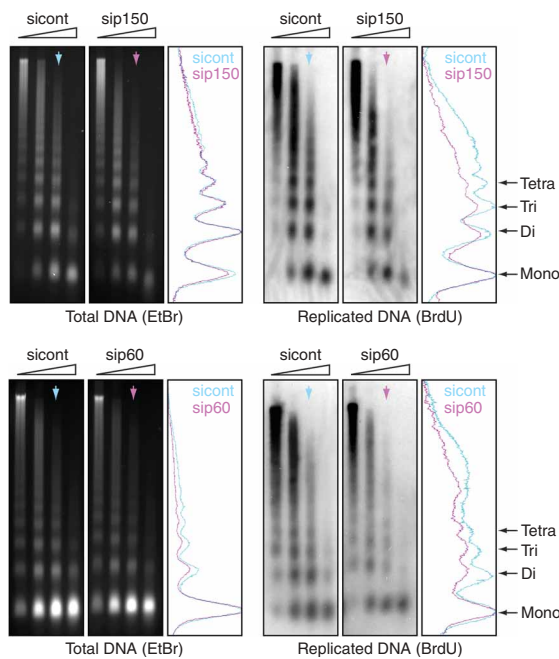


**Figure 2** Nucleosomal organization in p150- and p60-depleted cells. Analysis of MNase-digestion patterns of nuclei isolated from cells transfected with siRNA against p150 (above) or p60 (below) and corresponding control cells transfected with control siRNA (sicont). Total DNA (left) and corresponding BrdU-labeled replicated DNA (right) are shown. Densitometric profiles of the 2-min-digestion products (cyan and magenta arrows) from cells treated with control siRNA (cyan) or siRNA against p150 and p60 (magenta) are shown. Profiles are normalized to the peak of maximum intensity. Positions of the oligonucleosomes are indicated.

approach affects one subunit without affecting the other and that p150 could fulfill a function at replication sites independently of p60. We conclude that, in mouse cells, p150 (but not p60) is specifically required for progression beyond early S phase.

#### p150 depletion does not elicit detectable DNA damage

The S-phase block and impaired cell proliferation observed upon p150 depletion was previously attributed to the activation of the DNA damage checkpoint in human cells<sup>25,26</sup>. Indeed, when the function of CAF-1 is compromised, incorrect assembly of DNA into nucleosomes during replication might lead to the accumulation of excessive amounts of naked DNA, potentially prone to damage, which could trigger activation of 'general' DNA damage checkpoint pathways. However, according to this scenario, p60 depletion should produce a similar outcome for cell-cycle progression as p150 depletion, given that both subunits are crucial for *de novo* nucleosome assembly on naked DNA *in vitro*<sup>8,26,30</sup> and that depletion of either of them impaired CAF-1-mediated nucleosome assembly *in vitro* (Supplementary Fig. 1c). This is not what we observed (Supplementary Fig. 1c,d, and refs. 28,30). Thus, in our cellular model, impaired S-phase progression upon p150 depletion may not necessarily result from a defect in CAF-1 nucleosome assembly function, as initially assumed.

We examined the nucleosomal status of both total DNA and newly replicated DNA *in vivo* within p150- and p60-depleted cells by micrococcal nuclease (MNase) digestion. We observed a similar increase in nuclease sensitivity for both p150- and p60-depleted cells when compared to control, indicating that in the absence of CAF-1 *in vivo* nucleosomal organization was affected (Fig. 2). This is consistent with the loss of the nucleosome-assembly function of CAF-1 in p150- and p60-depleted cells (Supplementary Fig. 1c). Notably, a nucleosomal ladder was still detected in p150- and p60-depleted cells (Fig. 2), indicating that, *in vivo*, nucleosome assembly on replicated DNA can proceed to some extent without CAF-1. This suggests that a major exposure of naked DNA is unlikely and is consistent with undetectable DNA degradation in p150- and p60-depleted cells, as visualized by alkaline gel electrophoresis (Supplementary Fig. 2a online). It remained possible that low

amounts of naked DNA leading to DNA damage below our detection limits may still have been exposed and have elicited a 'general' DNA damage checkpoint. However, neither immunofluorescence (Supplementary Fig. 2b–d) nor western blot analysis (Supplementary Fig. 2e) detected increased phosphorylation of H2AX, p53 and Chk1, as indicators of checkpoint activation<sup>31–33</sup>, following p150 or p60 depletion. We thus conclude that DNA damage checkpoints were not activated to levels generally observed for S-phase arrest as a consequence of DNA damage<sup>33</sup>.

Therefore, under our experimental conditions, the failure of mouse cells to progress through S phase when p150 is depleted cannot be attributed to the activation of a 'general' DNA damage checkpoint as a consequence of defects in nucleosome assembly. Furthermore, given that either p60 or p150 depletion led to similar defects in nucleosome assembly *in vitro* (Supplementary Fig. 1c) and *in vivo* (Fig. 2), but that lack of p60 did not alter S phase, our data suggest that p150, in addition to its role in nucleosome assembly, has an additional role that influences progression of cells beyond early S phase.

#### Centromeric DNA is not replicated in p150-depleted cells

To gain insight into this possible role, we first analyzed possible defects in elongation during S phase. We used pulse-chase labeling with BrdU and biotinyl-16 dUTP (BiodU) to compare replication fork progression in p150-depleted and control cells. The spatial separation of the two labels into different foci is a direct reflection of the rate of replication elongation (Fig. 3a and Supplementary Methods online)<sup>18</sup>. Therefore, a reduced replication fork progression manifests as persistent colocalization of both labels. Persistent colocalization of BrdU and BiodU labeling in cells exposed to hydroxyurea, leading to replication arrest, validated that our assay efficiently revealed reduced replication fork progression (Supplementary Fig. 3a and Supplementary Methods online). Because p150-depleted cells arrest at the transition from early to mid-late S phase (Fig. 1c), only the early S-phase replication pattern could be monitored. For comparison of colocalization persistence, we therefore analyzed early S-phase patterns in p150-depleted and control cells. We found that, within the resolution limits of our approach, replication fork progression during early S phase was similar in p150-depleted and control cells, suggesting that defects in p150-depleted cells cannot relate to an impact on the global replication machinery (Fig. 3a, below). These data are in contrast to the response to hydroxyurea, in which early S-phase replication is affected (Supplementary Fig. 3a) without changing the proportion of S-phase replication profiles (Supplementary Fig. 3b). Taken together, these results suggest that the impaired S-phase progression in p150-depleted cells could reflect a defect beyond early S phase and specific to mid-late and/or late S phase.

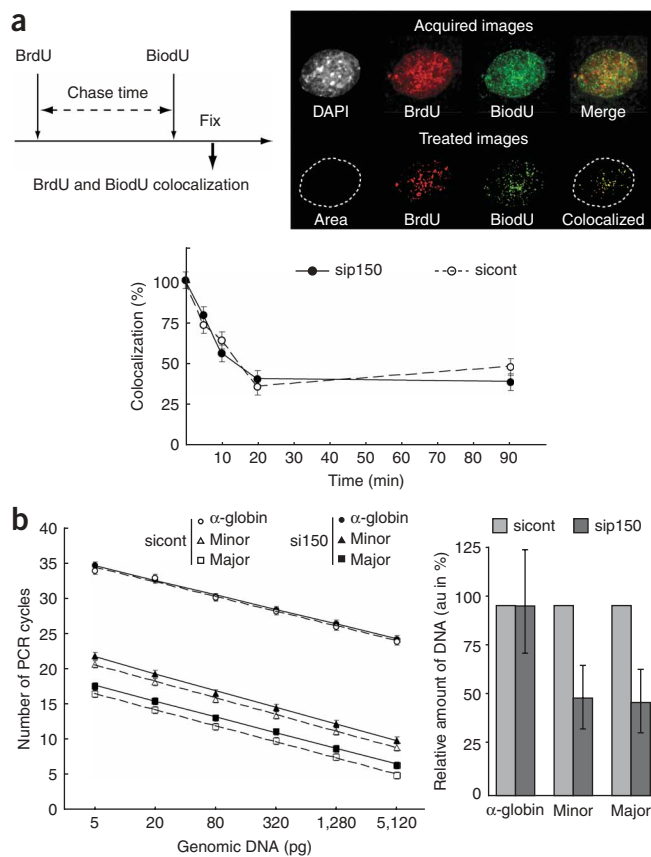
To investigate such replication defects, we focused our attention on satellite DNA sequences for which replication timing had already been documented in 3T3 cells<sup>7,23</sup>. Major satellite sequences in pericentric regions (enriched in HP1) first replicate in mid-late S phase followed by minor satellite sequences in centric regions (low HP1)<sup>7</sup>. Using

**Figure 3** Depletion of p150 does not affect the rate of DNA elongation but impairs centromeric DNA replication. (a) Above left, scheme of the elongation assay. Above right, illustration of the image treatment used to quantify the colocalization of BrdU (red) and BiodU (green; **Supplementary Fig. 3** and **Supplementary Methods**). Pixels with identical two-dimensional coordinates in the BrdU and BiodU channels (yellow) were scored as colocalized. Below, graph showing BrdU and BiodU colocalization as a function of chase time in cells transfected with control siRNA (sicont, dashed line) or siRNA against p150 (sip150, solid line). Data are normalized to 100% of colocalization at chase time = 0 min. Symbols indicate the mean and error bars indicate the s.d. ( $\pm 6$ ) from the analysis of 50 nuclei. (b) Genomic DNA purified from p150-depleted cells contains less major and minor satellite DNA than that of control cells. Left, graph shows the number of PCR cycles required to detect each target sequence (as indicated) as a function of the amount of genomic DNA purified from cells transfected with control siRNA (sicont, open symbols, dashed line) or cells transfected with siRNA against p150 (sip150, filled symbols, solid line). The symbols indicate the means and the error bars the s.d. ( $\pm 0.4$  cycles) of three independent experiments. Right, quantification of the amount of each DNA sequence ( $\alpha$ -globin, minor and major satellite sequences) in arbitrary units (au) in cells transfected with control siRNA (sicont, light shading) or siRNA against p150 (sip150, dark shading). The amounts are normalized to 100% for the control duplex and error bars indicate the s.d. corresponding to  $\pm 0.4$  PCR cycles.

real-time quantitative PCR, we measured the relative amounts of these satellite sequences using DNA extracted from control cells and p150-depleted cells. As an early-replicating control DNA sequence, we used the  $\alpha$ -globin gene<sup>34</sup>. An identical number of PCR cycles was required for amplification of the  $\alpha$ -globin gene from serially diluted DNA extracted from control and p150-depleted cells (**Fig. 3b**, left), consistent with the absence of a defect in replication fork progression for early S-phase patterns in p150-depleted cells (**Fig. 3a**). In contrast, amplification of the major and minor satellite sequences reproducibly required an additional cycle when using DNA from cells lacking p150 (**Fig. 3b**, left). Thus, we observed a two-fold reduction in major and minor satellite DNA in cells lacking p150 when compared to control cells (**Fig. 3b**, right). These data demonstrate that depletion of p150 does not affect replication of an early-replicating gene ( $\alpha$ -globin) but impairs replication of both pericentric and centric satellite DNA replicating in mid-late and late S phase, respectively. This is consistent with the decrease of mid-late and late-replication profiles when p150 is depleted (**Fig. 1c**). Furthermore, they strongly support the idea that loss of mid-late and late-replication patterns can be attributed to a true replication defect, rather than disruption of their spatial organization. We conclude that replication of pericentric and centric DNA specifically requires p150.

### Interaction of p150 with HP1 is required for S-phase progression

Depletion of p150 impaired replication of HP1-enriched heterochromatin, and p150 is the only subunit of CAF-1 that interacts with HP1 (ref. 21). This led us to hypothesize that the requirement of p150 for S-phase progression resides in the link between p150 and HP1 rather than in the nucleosome-assembly function of CAF-1. We thus investigated whether impairing the interaction between p150 and HP1, without affecting the ability of p150 to support histone deposition, is sufficient to cause an S-phase arrest similar to p150 depletion. The MIR domain of p150 (Mod-interacting region, PVVVL motif in mouse) is critical for interaction with HP1 (refs. 21,22) but dispensable for nucleosome assembly and interaction with known p150 partners including PCNA, p60 and MBD1 (refs. 8,20,35,36; **Fig. 4a**). We established 3T3 cell lines stably expressing GFP fusion constructs of wild-type p150 (GFPp150WT) and p150 mutants lacking the



PVVVL motif (GFPp150 $\Delta$ PVVVL) (**Fig. 4a**). Notably, these fusion proteins accumulate at replication foci and produce early, mid-late and late S-phase patterns, as visualized by GFP fluorescence (data not shown and **Supplementary Fig. 4a** online) and their expression did not affect the cell cycle (**Supplementary Fig. 4b**). We verified that, whereas GFPp150WT associates with endogenous HP1 like endogenous p150, GFPp150 $\Delta$ PVVVL does not (**Supplementary Fig. 4c**). However, both WT and  $\Delta$ PVVVL mutant GFPp150 fusion proteins were competent for nucleosome assembly (**Supplementary Fig. 4d**).

We then designed an siRNA targeting the 5' untranslated region (UTR) of the endogenous p150 in order to deplete the endogenous p150 without affecting the exogenous fusion proteins, whose mRNAs lack the 5' UTR, enabling us to generate cells dependent on the expression of the GFPp150WT or GFPp150 $\Delta$ PVVVL (**Fig. 4b,c**, combinations I and IV). In contrast, siRNA targeting p150 leads to depletion of both endogenous p150 and exogenous GFPp150 fusions (**Fig. 4b,c**, combinations III and VI). Notably, these GFPp150 fusions were expressed at levels comparable to endogenous p150 in each cell line (**Fig. 4c**).

When the endogenous p150 was specifically depleted (si' UTR), cells expressing the integrated GFPp150WT were not affected and behaved essentially like control cells (**Supplementary Fig. 4e**, 5' UTR, combination I). In contrast, cell proliferation was severely affected in cells expressing the GFPp150 $\Delta$ PVVVL (**Supplementary Fig. 4e**, 5' UTR, combination IV), similar to what is obtained upon depletion of both endogenous and exogenous p150 (**Supplementary Fig. 4e**, sip150, combinations III and VI). Thus, the region of p150 necessary for interaction with HP1 is crucial for cell proliferation.

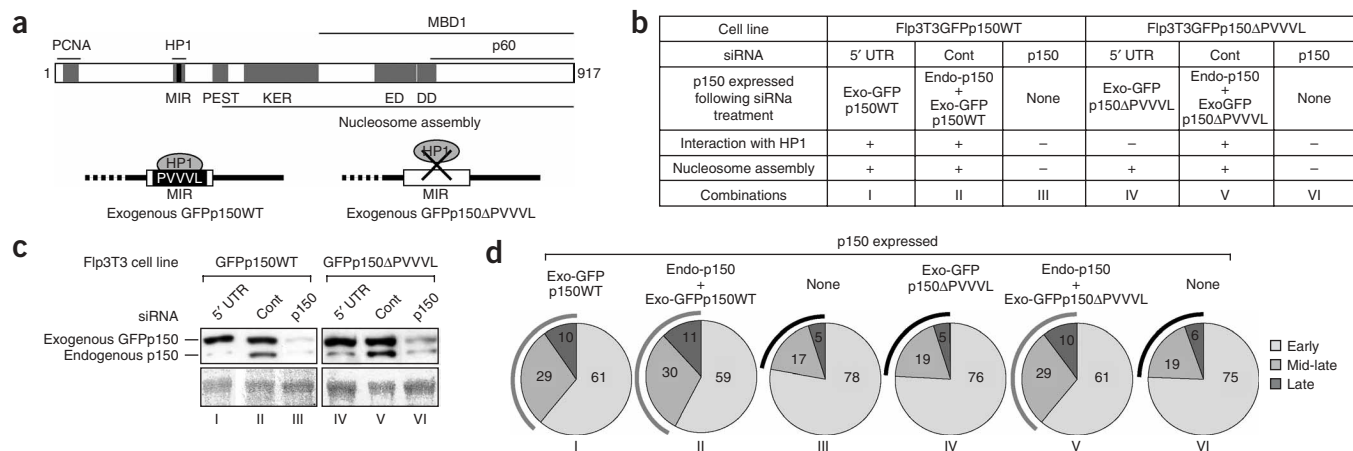


**Figure 4** Progression from early to mid-late S phase depends on interaction between p150 and HP1. **(a)** Above, schematic representation of the mouse p150 protein showing regions required for interaction with PCNA, HP1 proteins, p60, MBD1 and the region required for nucleosome assembly. The MIR, PEST, acidic KER/ED domains and the p150 dimerization domain (DD) are indicated in gray and the PVVVL motif in black. Below, schematic representation of the exogenous GFPp150WT (left) and GFPp150ΔPVVVL (right). The GFP moieties in the p150 fusion proteins are indicated as dotted lines. Interaction between HP1 (gray) and the PVVVL motif (black) in the MIR domain (rectangle) of GFPp150WT is shown. **(b)** Table showing the different combinations (I to VI) of cell lines stably expressing the GFP fusion proteins and siRNAs transfections such that cells express only: the exogenous GFPp150WT or exogenous GFPp150ΔPVVVL (si5' UTR, I and IV); endogenous p150 together with exogenous GFPp150 fusion proteins (siCont, II and V); no p150 (sip150, III and VI). Nucleosome assembly can be promoted (+) or not (-) by p150 (endogenous and/or GFP fusions (**Supplementary Fig. 4d**), and the ability of HP1 to interact (+) or not (-) with p150 (endogenous and/or GFP, **Supplementary Fig. 4c**) is indicated for each combination. **(c)** Western blot analysis of total cell extracts following transfection of the Flp3T3GFPp150WT and Flp3T3GFPp150ΔPVVVL cell lines with control siRNA (cont) or siRNA against 5' UTR (5' UTR) or p150 (p150). An anti-p150 antibody was used for detection. Ponceau staining of the membrane (below) is used as loading control. Roman numbers at the bottom correspond to the combinations described in **b**. **(d)** Pie charts showing quantitative analysis of the proportion of S-phase profiles scored based on PCNA immunostainings as in **Figure 1c**. Combination used for selective expression of exogenous GFPp150 fusion proteins and/or endogenous p150 is indicated in Roman numbers below. Numbers represent the mean of three independent experiments ( $n = 200$  S-phase nuclei per experiment) with s.d. identical to that detailed in **Figure 1c**.

We focused on adherent cells (48–72 h after transfection) in which we could monitor S-phase progression. Depletion of both endogenous and exogenous p150 resulted in an increase in early S-phase patterns and a decrease of the mid-late and late S-phase patterns when compared to control cells (**Fig. 4d**, compare combinations III and VI with II and V), as observed in 3T3 cells (**Fig. 1c**). The selective depletion of endogenous p150 in cells expressing GFPp150WT did not affect the normal proportion of S-phase patterns (**Fig. 4d**, compare combination I with II). In contrast, depletion of endogenous p150 in cells expressing GFPp150ΔPVVVL led to an alteration of S-phase patterns in a manner comparable to the effect of endogenous p150 depletion (**Fig. 4d**, compare combination IV with VI). Taken together, these data show that the GFPp150WT fusion protein can compensate for the loss of the endogenous p150, but the lack of the HP1-interaction domain in GFPp150ΔPVVVL prevents compensation of

the loss of endogenous p150, although GFPp150ΔPVVVL is proficient for nucleosome assembly. We thus conclude that, in 3T3 cells, the ability of p150 to support nucleosome assembly is not sufficient to ensure progression through mid-late and late S phase and rather that

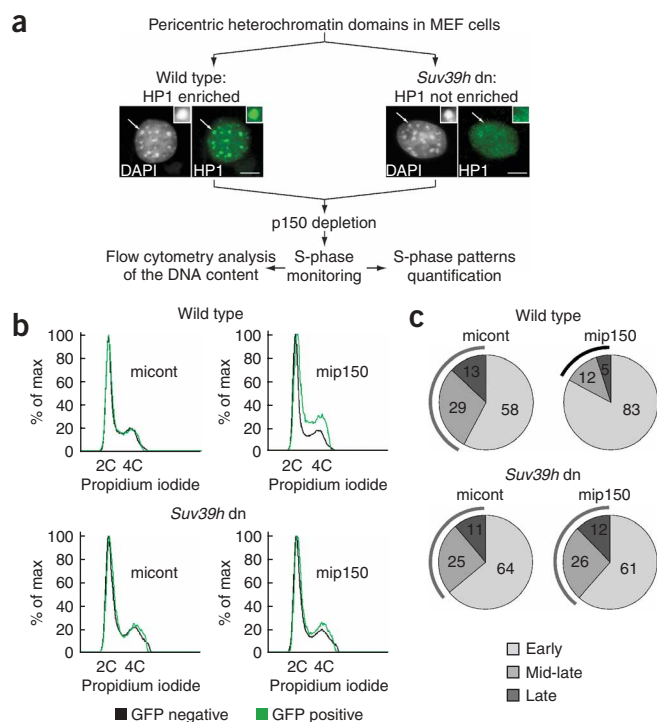


**Figure 5** S-phase progression is not perturbed in *Suv39h* dn MEF cells. **(a)** Experimental scheme showing the use of wild-type MEFs (left) with HP1 enrichment at pericentric heterochromatin domains or *Suv39h* dn MEFs (right) without HP1 enrichment at pericentric heterochromatin domains. Representative HP1 $\alpha$  and corresponding DAPI stainings are shown. Insets show two-fold magnifications of selected individual domains (arrows). Scale bar, 5  $\mu$ m. **(b)** Flow-cytometry analysis of the DNA content of wild-type MEFs (top) and *Suv39h* dn MEFs (bottom) transfected with miRNA control (micont, left) or miRNA targeting p150 (mip150, right). Profiles from GFP-negative cells (black) and GFP-positive cells (green) are overlaid. **(c)** Pie charts show quantitative analysis of the proportion of S-phase profiles scored based on PCNA immunostainings as in **Figure 1c**, in wild-type (top) and *Suv39h* dn (bottom) MEFs transfected as in **b**. Numbers represent the mean of two independent experiments ( $n = 150$  S-phase nuclei per experiment) with s.d. identical to that detailed in **Figure 1c**.

it is its ability to interact with HP1 that is a key limiting parameter at this stage of S phase.

### Requirement for p150 is alleviated in *Suv39* dn cells

We reasoned that, if the critical role of p150 is connected to its interaction with HP1, then reduction of HP1 concentration at pericentric domains should alleviate the requirement for p150 during S phase. We took advantage of mouse embryonic fibroblasts (MEFs) derived from *Suv39h* double-null mutant mice (*Suv39h* dn)<sup>37</sup> in which the lack of *Suv39h* histone H3K9 trimethylases leads to a loss of HP1 localization at pericentric heterochromatin domains<sup>38</sup> (Fig. 5a). Because we could not efficiently transfect MEFs with siRNA duplex, we transfected cells with a plasmid encoding a microRNA (miRNA) to downregulate p150, and GFP to enable identification of the transfected cells expressing the p150 miRNA. To validate this approach, we verified by immunofluorescence that 72 h after transfection 90% of GFP-positive MEFs or 3T3 cells were depleted of p150 (Supplementary Fig. 5a,b online) and that 3T3 cells depleted by this method showed the same phenotype as those depleted by siRNA (Supplementary Fig. 5d,e). Flow cytometry analysis of the DNA content revealed that in wild-type MEFs p150 depletion resulted in S-phase arrest. In contrast, *Suv39h* dn MEFs depleted of p150 did not show any changes when compared to nontransfected cells or cells transfected with the plasmid expressing the miRNA control (Fig. 5b). Furthermore, changes in the proportion of S-phase patterns found for the wild-type MEFs were not detected in the *Suv39h* dn MEFs (Fig. 5c). These data further support the idea that in mouse cells the crucial role of p150 for S-phase progression is directly linked to the presence of HP1 enrichment at pericentric heterochromatin domains.

### DISCUSSION

Our results reveal that the p150 subunit of CAF-1 possesses a unique function that is crucial for S-phase progression in mouse cells. This function, distinct from the known property of the whole CAF-1 complex to promote histone deposition, relies on a key HP1–p150 interaction module, underlining the fact that the CAF-1 complex should be considered not only as a histone-deposition complex (which requires all three subunits), but also as a multitasking factor that integrates information via individual subunits. We propose that p150 provides a novel type of control at regions enriched in HP1, and thus we call it a built-in heterochromatin control of replication. By efficiently coordinating HP1 dynamics and replication fork progression, this mechanism would ensure reproduction of specialized chromatin structures present at key regions of the genome.

Most importantly, our data reveal that in mouse cells, even if CAF-1 is able to promote nucleosome assembly, lack of interaction between p150 and HP1 is critical and prevents S-phase progression. Formally, the defect could result from impaired preinitiation, initiation or elongation events. Given that p150 recruitment to replication foci is supposed to depend on its interaction with PCNA<sup>19,20</sup>, and that loading of PCNA occurs post-initiation<sup>39</sup>, we favor the idea of a requirement for p150 in elongation. We cannot, however, exclude the possibility that p150 could be recruited earlier by an unknown mechanism.

Regions in the genome with complex chromatin organization could potentially impose structural constraints that, if not relieved, prevent replication fork progression without possible bypass. In HP1-rich regions, the unique properties of p150 could be used to facilitate passage of the replication fork. This would involve displacing HP1 from the chromatin ahead of the replication fork and transferring it onto newly replicated DNA behind the fork, in order to transiently

and locally relieve constraints that are imposed or maintained by HP1. Such an acceptor/donor role for p150 is supported by the finding that the HP1–CAF-1 complex is highly dynamic *in vivo*<sup>23</sup> and that CAF-1 promotes deposition of HP1 $\beta$  on nascent chromatin *in vitro*<sup>21</sup>.

The importance of this additional function of p150 for S-phase progression and ultimately cellular viability is likely to depend on the cell type and the organism, considering in each case the features of their heterochromatin. The requirement of p150 for the replication of HP1-rich regions could be highest during early development in mice. Indeed, knockout of p150 is lethal during mouse preimplantation development at a time when HP1-enriched pericentric heterochromatin domains are normally established in clusters to form DAPI-dense dot structures after the 8–16-cell stage<sup>40</sup>. In the context of cells with less complex heterochromatin domains, such p150-dependent function would not necessarily be so crucial. For example, in *Arabidopsis thaliana*, centromeric domains are not clustered, and CAF-1 mutants are viable<sup>41</sup>. The same could apply to chicken DT40 cells, in which the interaction of p150 with HP1 in DT40 cells is not required for cell viability<sup>27</sup>. One should note, however, that in both organisms lack of p150 results in mitotic and heterochromatin defects<sup>27,42,43</sup>, still in line with a role of p150 in heterochromatin. The biological context (organism, cell line and developmental stage) could determine the extent to which defects in nucleosomal organization and/or the control of the replication of HP1-rich domains will affect viability.

In chicken, mouse and human tissue-culture cells, depletion of CAF-1 affects *in vivo* nucleosomal organization (refs. 27,30 and this study) and this can cause DNA damage, checkpoint activation and cell death<sup>25,26</sup>. This could explain why the lack of p150 or altered p150 function can prove to be lethal even in the absence of clustered centromeric HP1 domains in DT40 cells<sup>27</sup>, human cells<sup>25,26</sup> and early (before the mid-blastula transition (MBT) stage) developing *Xenopus* embryos<sup>44</sup>. In the case of mouse cells where pericentric heterochromatin domains from several chromosomes associate in clusters, replication of these HP1-rich domains could create a higher demand for the p150–HP1 interaction module, forming a barrier preventing S-phase progression in absence of this module. This would occur before the accumulation of defects in nucleosome assembly, which would in turn lead to activation of a ‘classical’ DNA-based checkpoint and S-phase arrest. One could also envisage a higher tolerance to the lack of CAF-1-mediated nucleosome assembly as a result of compensating nucleosome-assembly activities, as in *S. cerevisiae*, where CAF-1 is not essential<sup>45–47</sup>.

Within the limits of detection of the assays, we did not observe a ‘general’ DNA damage checkpoint activation in the S-phase arrest following p150 depletion. This excludes the possibility that the trigger for the S-phase arrest relates to sensing DNA damage directly or indirectly<sup>48</sup>. This is reminiscent of a situation in *S. pombe* where the replication fork barrier *RTS1* can block replication fork progression without involving a classical DNA-based checkpoint activation<sup>49,50</sup>. An S-phase arrest resulting from steric hindrance ahead of the replication fork that physically blocks progression would prevent uncoupling between the DNA-unwinding and polymerase activities at the fork, and thus prevent the generation of replication factor A-coated single-stranded DNA<sup>51</sup> as a signal for checkpoint activation<sup>52</sup>. In the case of heterochromatin domains, such a control would prevent exposure of long stretches of repetitive DNA during replication that would be prone to aberrant recombination and pose a threat to genome stability<sup>3</sup>. Notably, in addition to affecting regions enriched in HP1, our data reveal that replication of the late-replicating minor satellite DNA repeats at which HP1 does not accumulate<sup>7</sup> are also affected when p150 is depleted, suggesting that a mid-late S-phase

replication defect impacts on subsequent replication events possibly by inhibiting late-replication firing<sup>53,54</sup>, but without a classical checkpoint activation.

Notably, S phase is delayed in response to depletion of the histone chaperone Asf1 without classical DNA-based checkpoint activation<sup>55</sup>. In this case, Asf1, via an interaction with the putative helicase MCM2-7 and histones, would ensure coordination of parental nucleosome disruption ahead of the fork and reassembly behind with replication fork progression<sup>55</sup>. At pericentric heterochromatin, p150 may have a role reminiscent of that of Asf1 to coordinate replication fork progression and HP1 dynamics ahead and behind the fork through its interaction with PCNA and HP1. One could envisage that progression of the replication fork through chromatin requires several interaction modules, dedicated to specific chromatin components and/or organization. These interaction modules could provide a means of controlling S-phase progression at the level of chromatin and be able to delay or arrest S phase independently of a DNA-based checkpoint.

In conclusion, our data enabled us to reveal the importance of an HP1-p150/CAF1 module to promote replication of HP1-rich regions in mouse cells. We propose that it can contribute to a particular replication control, in addition to the classical DNA-based checkpoints, that would operate at key chromosomal regions as a 'built-in' lock for heterochromatin replication. In this scheme, the complex organization of constitutive heterochromatin, central to centromere function, through its very components (that is, HP1 proteins), would create a barrier that p150 could help to overcome, and thus control S-phase progression. This kind of S-phase control would be advantageous to prevent subsequent aberrant mitosis. Although this is the most simple explanation for our data, we cannot exclude the possibility that, in addition to the release of steric hindrance imposed by the chromatin organization, CAF-1 may also contribute to other forms of S-phase control involving chromatin-based checkpoints<sup>56</sup>. Whether this novel type of control can apply to other regions of the genome such as telomeres, where steric hindrance problems may also arise, and whether it can be exploited to control cell proliferation will need further investigations.

## METHODS

**Cells.** 3T3 (US National Institutes of Health (NIH)) and MEF cells were grown in DMEM (Gibco BRL) containing 10% (v/v) FCS at 37 °C and 5% CO<sub>2</sub>. We used donor calf serum instead of FCS for Flp3T3 (Invitrogen). We inserted cDNAs encoding GFPp150WT and GFPp150ΔPVVVL<sup>21</sup> into pcDNA5FRT plasmid (Invitrogen) to generate Flp3T3 cells stably expressing the GFPp150 fusion proteins (Flp3T3GFPp150WT and Flp3T3GFPp150ΔPVVVL). As a positive control for checkpoint activation, we exposed cells to 3 mM hydroxyurea for 1.5 h. We prepared total cell extract by resuspending cells in Laemmli SDS-PAGE sample loading buffer.

**siRNA and miRNA treatments.** We synthesized and transfected siRNA duplexes as described<sup>23</sup>. Plasmids expressing the control miRNA or the miRNA targeting p150 were constructed according to the Block-iT™ Pol II miR RNAi system (Invitrogen) and transfected using the AMAXA system. We carried out analyses between 48 h and 72 h after transfection. The sequences of the siRNA duplexes were as follows: sip150, 5'-AAGGAGAAGGCGGAGAAGCAG-3'; sip60, 5'-AAAGGUGAACUUGGCAUACCU-3'; si5'UTR, 5'-AAGCCUGAGC CGCCGCCGCCG-3'; sicont, 5'-AAGCUGGAGUACAACUACAACCCUGUC UC-3' (targets GFP). The control siRNA used in experiments involving GFP fusion proteins (Fig. 4 and Supplementary Fig. 4) was the scrambled II duplex from Dharmacon (5'-AAGCGCGCUUUGUAGGAUUCG-3').

**Immunochemistry and image acquisition.** Cells were processed for immunostaining as described<sup>23</sup>. For simultaneous visualization of p150 staining and GFP, cells were not extracted before fixation. For quantification of early,

mid-late and late S-phase cells, more than 300 nuclei from at least three independent experiments were scored. We carried out pulse-chase-labeling experiments with BrdU and BiodU as described<sup>18</sup>. A DMR-HC (Leica) epifluorescence microscope equipped with a ×63 objective lens and a chilled CCD camera (CoolSnap Fx, Photometrics) was used for image acquisition. Analysis of the colocalization of BrdU and BiodU incorporation was performed using Metamorph software (Universal Imaging); see numerical treatment in **Supplementary Methods**.

**Micrococcal nuclease digestion and BrdU detection.** We carried out digestion with MNase (30 s, 1 min, 2 min and 5 min) on nuclei isolated from cells pulsed for 30 min with 40 μM BrdU. Digestion products were analyzed by agarose gel electrophoresis. Total DNA was visualized by ethidium bromide staining, and BrdU-labeled replicated DNA was visualized by immunodetection of BrdU as described<sup>57</sup>.

**Antibodies.** See description in **Supplementary Methods**.

**Real-time quantitative PCR.** We performed real-time quantitative PCR reactions on DNA extracted from siRNA-treated cells with a Light Cycler PCR machine (Roche) using the following primer pairs: α-globin forward, 5'-AAGGGGAGCAGAGGCATCA-3'; α-globin reverse, 5'-AGGGCTTGGGAG GGACTG-3' (ref. 34); minor satellite repeat forward, 5'-GAAAATGATAAAAA CCACAC-3'; minor satellite repeat reverse, 5'-ACTCATTGATATACACTGTT-3'; major satellite repeat forward, 5'-AAATACACACTTTAGGACG-3'; major satellite repeat reverse 5'-TCAAGTGGATGTTTCTCATT-3'. The number of cycles, corresponding to the start of the log-linear phase of the PCR amplification (crossing point), was determined using the Light Cycler software.

*Note: Supplementary information is available on the Nature Structural & Molecular Biology website.*

## ACKNOWLEDGMENTS

We thank J. Haber for critical reading of the manuscript and members of our unit for discussions (D. Ray-Gallet, S. Polo, M.K. Ray and J. Chow); S. Huart for quantitative co-localization analyses; N. Murzina (Department of Biochemistry, University of Cambridge) and A. Verreault (IRIC, Université de Montréal, Canada) for the gift of mouse GFPp150 constructs; M. Moné for establishing 3T3Flp cell lines stably expressing GFPp150 proteins (Institute of Molecular Cell Biology, Faculty for Earth and Life Sciences, Vrije Universiteit, Amsterdam). A.G. received support from Délégation Générale pour l'Armement (DGA/DSP/STTC/DT/SH) and Association pour la Recherche sur le Cancer. A.J.L.C. received support from la Ligue Nationale Contre le Cancer. This work was supported by the Ligue Nationale Contre le Cancer (Equipe labellisée la Ligue), the Institut Curie PIC Programs ('Retinoblastome' and 'Replication, Instabilité chromosomique et cancer'), the European Commission Network of Excellence Epigenome (LSHG-CT-2004-503433), ACI-2004-Cancéropole IdF 'Breast cancer and epigenetics, ANR 'CenRNA' NT05-4\_42267 and ANR 'FaRC', PCV06\_142302.

## AUTHOR CONTRIBUTIONS

J.-P.Q. and G.A. conceived and designed the experiments; J.-P.Q., A.G., A.J.L.C. and D.R. performed the experiments; J.-P.Q., A.G., A.J.L.C., D.R. and G.A. analyzed the data; J.-P.Q., A.J.L.C. and G.A. wrote the paper.

Published online at <http://www.nature.com/nsmb/>

Reprints and permissions information is available online at <http://npg.nature.com/reprintsandpermissions/>

- Luger, K., Mader, A.W., Richmond, R.K., Sargent, D.F. & Richmond, T.J. Crystal structure of the nucleosome core particle at 2.8 Å resolution. *Nature* **389**, 251–260 (1997).
- Grewal, S.I. & Jia, S. Heterochromatin revisited. *Nat. Rev. Genet.* **8**, 35–46 (2007).
- Peng, J.C. & Karpen, G.H. Epigenetic regulation of heterochromatic DNA stability. *Curr. Opin. Genet. Dev.* **18**, 204–211 (2008).
- Gilbert, N. *et al.* Formation of facultative heterochromatin in the absence of HP1. *EMBO J.* **22**, 5540–5550 (2003).
- Maison, C. & Almouzni, G. HP1 and the dynamics of heterochromatin maintenance. *Nat. Rev. Mol. Cell Biol.* **5**, 296–304 (2004).
- Kalitsis, P. & Choo, K.H.A. Centromere DNA of higher eukaryotes. in *The Centromere* (ed. Choo, K.H.A.) 97–140 (Oxford Univ. Press, New York, 1997).
- Guenatri, M., Bailly, D., Maison, C. & Almouzni, G. Mouse centric and pericentric satellite repeats form distinct functional heterochromatin. *J. Cell Biol.* **166**, 493–505 (2004).

8. Kaufman, P.D., Kobayashi, R., Kessler, N. & Stillman, B. The p150 and p60 subunits of chromatin assembly factor I: a molecular link between newly synthesized histones and DNA replication. *Cell* **81**, 1105–1114 (1995).
9. Polo, S.E. & Almouzni, G. Chromatin assembly: a basic recipe with various flavours. *Curr. Opin. Genet. Dev.* **16**, 104–111 (2006).
10. Groth, A., Rocha, W., Verreault, A. & Almouzni, G. Chromatin challenges during DNA replication and repair. *Cell* **128**, 721–733 (2007).
11. Cheutin, T. *et al.* Maintenance of stable heterochromatin domains by dynamic HP1 binding. *Science* **299**, 721–725 (2003).
12. Festenstein, R. *et al.* Modulation of heterochromatin protein 1 dynamics in primary mammalian cells. *Science* **299**, 719–721 (2003).
13. Karpen, G.H. & Allshire, R.C. The case for epigenetic effects on centromere identity and function. *Trends Genet.* **13**, 489–496 (1997).
14. Folco, H.D., Pidoux, A.L., Urano, T. & Allshire, R.C. Heterochromatin and RNAi are required to establish CENP-A chromatin at centromeres. *Science* **319**, 94–97 (2008).
15. Verreault, A., Kaufman, P.D., Kobayashi, R. & Stillman, B. Nucleosome assembly by a complex of CAF-1 and acetylated histones H3/H4. *Cell* **87**, 95–104 (1996).
16. Smith, S. & Stillman, B. Purification and characterization of CAF-I, a human cell factor required for chromatin assembly during DNA replication *in vitro*. *Cell* **58**, 15–25 (1989).
17. Krude, T. Chromatin assembly factor 1 (CAF-1) colocalizes with replication foci in HeLa cell nuclei. *Exp. Cell Res.* **220**, 304–311 (1995).
18. Taddei, A., Roche, D., Sibarita, J.B., Turner, B.M. & Almouzni, G. Duplication and maintenance of heterochromatin domains. *J. Cell Biol.* **147**, 1153–1166 (1999).
19. Shibahara, K. & Stillman, B. Replication-dependent marking of DNA by PCNA facilitates CAF-1-coupled inheritance of chromatin. *Cell* **96**, 575–585 (1999).
20. Moggs, J.G. *et al.* A CAF-1/PCNA mediated chromatin assembly pathway triggered by sensing DNA damage. *Mol. Cell Biol.* **20**, 1206–1218 (2000).
21. Murzina, N., Verreault, A., Laue, E. & Stillman, B. Heterochromatin dynamics in mouse cells: interaction between chromatin assembly factor 1 and HP1 proteins. *Mol. Cell* **4**, 529–540 (1999).
22. Thiru, A. *et al.* Structural basis of HP1/PXVXL motif peptide interactions and HP1 localisation to heterochromatin. *EMBO J.* **23**, 489–499 (2004).
23. Quivy, J.P. *et al.* A CAF-1 dependent pool of HP1 during heterochromatin duplication. *EMBO J.* **23**, 3516–3526 (2004).
24. Tagami, H., Ray-Gallet, D., Almouzni, G. & Nakatani, Y. Histone H3.1 and H3.3 complexes mediate nucleosome assembly pathways dependent or independent of DNA synthesis. *Cell* **116**, 51–61 (2004).
25. Ye, X. *et al.* Defective S phase chromatin assembly causes DNA damage, activation of the S phase checkpoint, and S phase arrest. *Mol. Cell* **11**, 341–351 (2003).
26. Hoek, M. & Stillman, B. Chromatin assembly factor 1 is essential and couples chromatin assembly to DNA replication *in vivo*. *Proc. Natl. Acad. Sci. USA* **100**, 12183–12188 (2003).
27. Takami, Y., Ono, T., Fukagawa, T., Shibahara, K. & Nakayama, T. Essential role of chromatin assembly factor-1-mediated rapid nucleosome assembly for DNA replication and cell division in vertebrate cells. *Mol. Biol. Cell* **18**, 129–141 (2007).
28. Polo, S.E., Roche, D. & Almouzni, G. New histone incorporation marks sites of UV repair in human cells. *Cell* **127**, 481–493 (2006).
29. Dimitrova, D.S. & Berezney, R. The spatio-temporal organization of DNA replication sites is identical in primary, immortalized and transformed mammalian cells. *J. Cell Sci.* **115**, 4037–4051 (2002).
30. Nabatiyan, A. & Krude, T. Silencing of chromatin assembly factor 1 in human cells leads to cell death and loss of chromatin assembly during DNA synthesis. *Mol. Cell Biol.* **24**, 2853–2862 (2004).
31. Tibbetts, R.S. *et al.* A role for ATR in the DNA damage-induced phosphorylation of p53. *Genes Dev.* **13**, 152–157 (1999).
32. Paull, T.T. *et al.* A critical role for histone H2AX in recruitment of repair factors to nuclear foci after DNA damage. *Curr. Biol.* **10**, 886–895 (2000).
33. Bartek, J. & Lukas, J. DNA damage checkpoints: from initiation to recovery or adaptation. *Curr. Opin. Cell Biol.* **19**, 238–245 (2007).
34. Azuara, V. *et al.* Heritable gene silencing in lymphocytes delays chromatid resolution without affecting the timing of DNA replication. *Nat. Cell Biol.* **5**, 668–674 (2003).
35. Reese, B.E., Bachman, K.E., Baylin, S.B. & Rountree, M.R. The methyl-CpG binding protein MBD1 interacts with the p150 subunit of chromatin assembly factor 1. *Mol. Cell Biol.* **23**, 3226–3236 (2003).
36. Sarraf, S.A. & Stancheva, I. Methyl-CpG binding protein MBD1 couples histone H3 methylation at lysine 9 by SETDB1 to DNA replication and chromatin assembly. *Mol. Cell* **15**, 595–605 (2004).
37. Peters, A.H. *et al.* Loss of the Suv39h histone methyltransferases impairs mammalian heterochromatin and genome stability. *Cell* **107**, 323–337 (2001).
38. Maison, C. *et al.* Higher-order structure in pericentric heterochromatin involves a distinct pattern of histone modification and an RNA component. *Nat. Genet.* **30**, 329–334 (2002).
39. Maga, G., Stucki, M., Spadari, S. & Hubscher, U. DNA polymerase switching: I. Replication factor C displaces DNA polymerase  $\alpha$  prior to PCNA loading. *J. Mol. Biol.* **295**, 791–801 (2000).
40. Houliard, M. *et al.* CAF-1 is essential for heterochromatin organization in pluripotent embryonic cells. *PLoS Genet.* **2**, e181 (2006).
41. Kaya, H. *et al.* FASCIATA genes for chromatin assembly factor-1 in *Arabidopsis* maintain the cellular organization of apical meristems. *Cell* **104**, 131–142 (2001).
42. Schonrock, N., Exner, V., Probst, A., Gruissem, W. & Hennig, L. Functional genomic analysis of CAF-1 mutants in *Arabidopsis thaliana*. *J. Biol. Chem.* **281**, 9560–9568 (2006).
43. Kirik, A., Pecinka, A., Wendeler, E. & Reiss, B. The chromatin assembly factor subunit FASCIATA1 is involved in homologous recombination in plants. *Plant Cell* **18**, 2431–2442 (2006).
44. Quivy, J.P., Grandi, P. & Almouzni, G. Dimerization of the largest subunit of chromatin assembly factor 1: importance *in vitro* and during *Xenopus* early development. *EMBO J.* **20**, 2015–2027 (2001).
45. Kaufman, P.D., Kobayashi, R. & Stillman, B. Ultraviolet radiation sensitivity and reduction of telomeric silencing in *Saccharomyces cerevisiae* cells lacking chromatin assembly factor I. *Genes Dev.* **11**, 345–357 (1997).
46. Enomoto, S., McCune-Zierath, P., Geraminejad, M., Sanders, M. & Berman, J. Rlf2, a subunit of yeast chromatin assembly factor-1, is required for telomeric chromatin function *in vivo*. *Genes Dev.* **11**, 358–363 (1997).
47. Kats, E.S., Albuquerque, C.P., Zhou, H. & Kolodner, R.D. Checkpoint functions are required for normal S-phase progression in *Saccharomyces cerevisiae* RCAF- and CAF-1-defective mutants. *Proc. Natl. Acad. Sci. USA* **103**, 3710–3715 (2006).
48. Tercero, J.A., Longhese, M.P. & Diffley, J.F. A central role for DNA replication forks in checkpoint activation and response. *Mol. Cell* **11**, 1323–1336 (2003).
49. Lambert, S., Watson, A., Sheedy, D.M., Martin, B. & Carr, A.M. Gross chromosomal rearrangements and elevated recombination at an inducible site-specific replication fork barrier. *Cell* **121**, 689–702 (2005).
50. Ahn, J.S., Osman, F. & Whitby, M.C. Replication fork blockage by RTS1 at an ectopic site promotes recombination in fission yeast. *EMBO J.* **24**, 2011–2023 (2005).
51. Byun, T.S., Pacek, M., Yee, M.C., Walter, J.C. & Cimprich, K.A. Functional uncoupling of MCM helicase and DNA polymerase activities activates the ATR-dependent checkpoint. *Genes Dev.* **19**, 1040–1052 (2005).
52. Zou, L. & Elledge, S.J. Sensing DNA damage through ATRIP recognition of RPA-ssDNA complexes. *Science* **300**, 1542–1548 (2003).
53. Bartek, J., Lukas, C. & Lukas, J. Checking on DNA damage in S phase. *Nat. Rev. Mol. Cell Biol.* **5**, 792–804 (2004).
54. Ben-Yehoyada, M., Gautier, J. & Dupre, A. The DNA damage response during an unperturbed S-phase. *DNA Repair (Amst)* **6**, 914–922 (2007).
55. Groth, A. *et al.* Regulation of replication fork progression through histone supply and demand. *Science* **318**, 1928–1931 (2007).
56. Ye, X. & Adams, P.D. Coordination of S-phase events and genome stability. *Cell Cycle* **2**, 185–187 (2003).
57. Poot, R.A. *et al.* The Williams syndrome transcription factor interacts with PCNA to target chromatin remodelling by ISWI to replication foci. *Nat. Cell Biol.* **6**, 1236–1244 (2004).